Supplementary Materials for

All-optical temporal integration mediated by subwavelength heat antennas

Yi Zhang[1]†, Nikolaos Farmakidis[1]†, Ioannis Roumpos[2]†, Miltiadis Moralis-Pegios[3], Apostolos Tsakyridis[3], June Sang Lee[1], Bowei Dong[1], Yuhan He[1], Samarth Aggarwal[1], Nikos Pleros[3]* and Harish Bhaskaran[1]*

Corresponding authors: harish.bhaskaran@materials.ox.ac.uk, npleros@csd.auth.gr

1. Simulation of spectral-selective absorption

This spectral-selective absorption effect is illustrated using finite difference time domain simulations (FDTD, Lumerical solutions) in fig. S1A. Here, the spatial field distribution in a silicon rib waveguide with absorptive titanium antennas on top shows periodic nodes and antinodes when coherent light is coupled in counterpropagating directions. For two antiphase wavelengths λ_1 and λ_2 the field at the antenna shows a maximum and a minimum respectively (fig. S1B, C). This wavelength selectivity is reflected in the absorption profiles (fig. S1D), where we calculate the total power absorbed by the antenna by integrating over the height of the structure. Here the total absorption experienced by λ_1 is 17 times higher than that of λ_2, where the structure is nearly transparent; any loss at λ_2 results from the finite size of the antenna.

As shown in Fig. S1E, F, after sending a 1-mW pulse with 500 ns width, the temperature between two antennas can be raised to 325.5 K with input λ_1, while its counterpart with input λ_2 remains around room temperature (301.1 K). This demonstrates the spatial non-locality of the thermo-optic effect induced by power absorption in nano-antennas. It also indicates low optical loss for wavelengths that do not overlap with the nano-antennas, thereby confirming the non-reciprocal behavior predicted by our design.

2. Pump at the non-absorptive wavelength

We changed the control line to the even-mode-resonant wavelength with similar transmission and repeated the process above to collect spectrums around the odd-mode-resonant peak as shown in the fig. S2A. Pumping at the probe signal (even-mode-resonant wavelength) has a weaker effect on shifting the spectrum at 0.0087 π/mW (fig. S2B) compared with 0.04 π/mW while pumping at the control signal (odd-mode-resonant wavelength), which reconfirms the low absorption at the probe signal and non-reciprocal operation proposed theoretically above.

3. Response characterization & leaky integrator

The modulation results on the probe signal transmission with different control signal pulse width are shown in fig. S6A, which has a response similar to the output of a leaky integrator due to the slow heat dissipation process.

In a leaky integrator, if we define y(t) as the output of this system at any time t,

$$y(t) \propto e^{-\frac{t}{\tau}}$$

The impulse response of a leaky integrator decays exponentially, in which the leak time constant (τ) defines how quickly the integrator "forgets" past inputs due to the leakage and determines the integration window of the system. τ is typically defined as the time it takes to decay to

approximately 1/e of its initial value when the input is removed. In our case, therefore, we estimate the time constant with device response to a 200-ns step input in fig. S6A, when the device response reaches the steady state. Fig.S6B shows a zoomed response characterization at 200 ns control pulse width and its extracted time constant (τ) is 130 ns, indicating a theoretical integration window where data can be added up before being 'forgotten', i.e. 'leaked'.

4. Accumulation of optical signals over wavelength with programmable transfer functions

In addition to the demonstration of linear summation of incoherent control signals and all-optical non-linear operation to the integrated time-multiplexed signals, we proceed to vary the wavelength of probe signals as discussed in the main text and successfully applied different activation functions to the incoherent summation results (fig. S8).

Fig. S1.

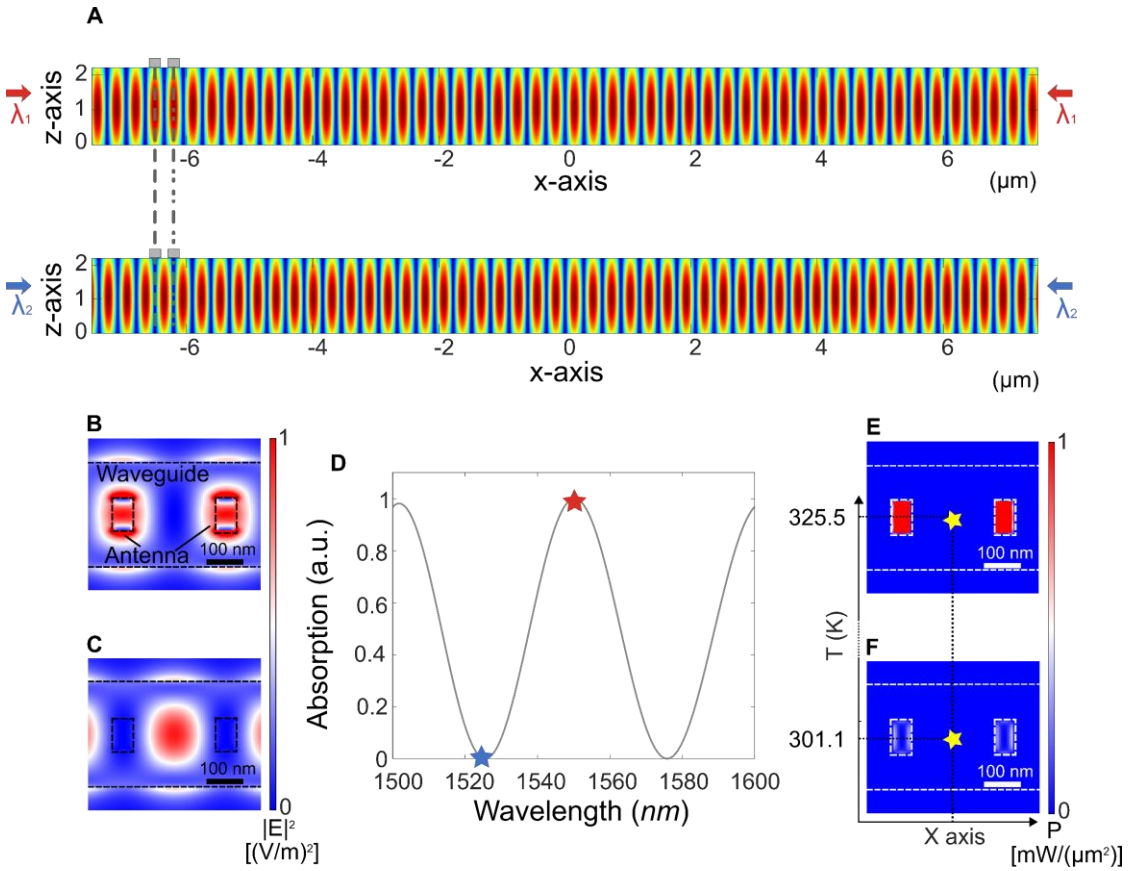

Fig. S1. Across-wavelength photon interactions via the thermo-optic effect. (**A**) Input light with equal intensities are sent into silicon waveguide from opposite directions. Two absorptive nano-antennas are designed to spatially match the anti-nodes of light λ_1 (1550.3 nm) (top) while overlapping with the nodes of light λ_2 (1525.6 nm) (bottom). (**B**, **C**) Normalized E-field of different wavelengths at the antennas. Titanium antennas of 20 nm thickness, 50 nm width and 250 nm length are placed on a rib waveguide with 500 nm width in the simulation. (**B**) Two absorptive nano-antennas are designed to spatially match the anti-nodes of λ_1, (**C**) while overlapping with the nodes of λ_2. (**D**) Here the total absorption experienced by λ_1 is 17 times higher than that of $\lambda_2$where the structure is nearly transparent. (**E**, **F**) Power absorbed per unit area by antennas with 1-mW input power. Inset Fig. indicates that heat generated by the absorption of light in the antenna region raises the temperature (K) of the surrounding waveguide, generated with *Lumerical* HEAT.

Fig. S2.

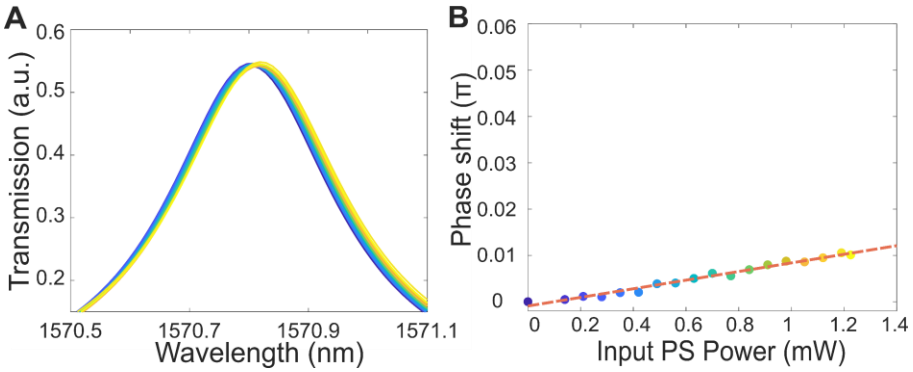

Fig. S2. Spectral response characterization with modulating probe signal. (**A**) Spectral response collected at odd mode modulated by even mode. (**B**) Pump at even mode has a weak effect at 0.0087 π/mW.

Fig. S3.

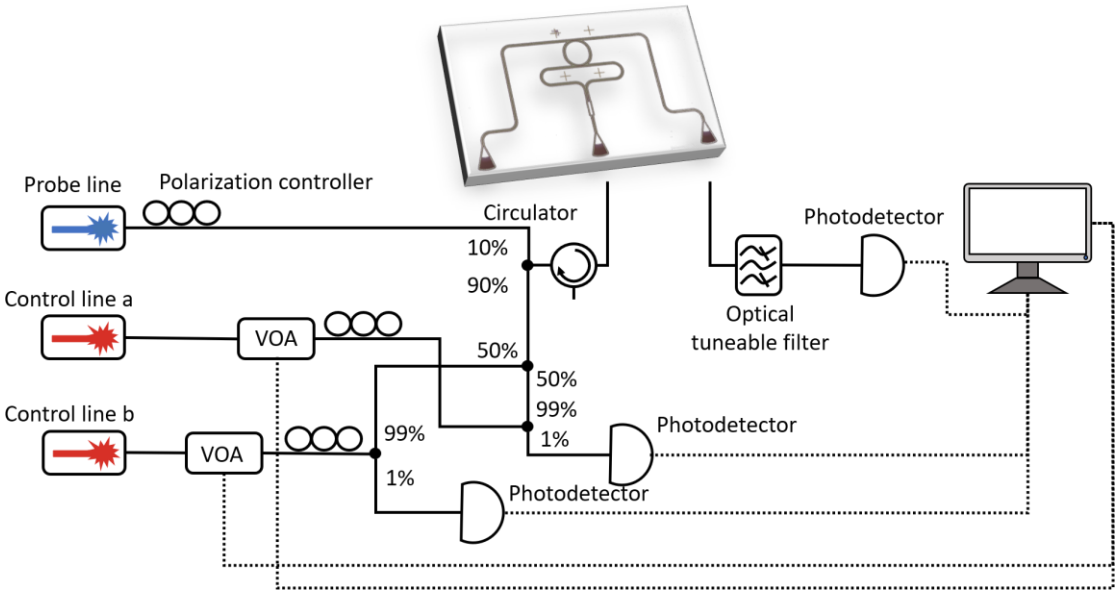

Fig. S3. Experiment set-up for accumulation operations across wavelengths.

Fig. S4.

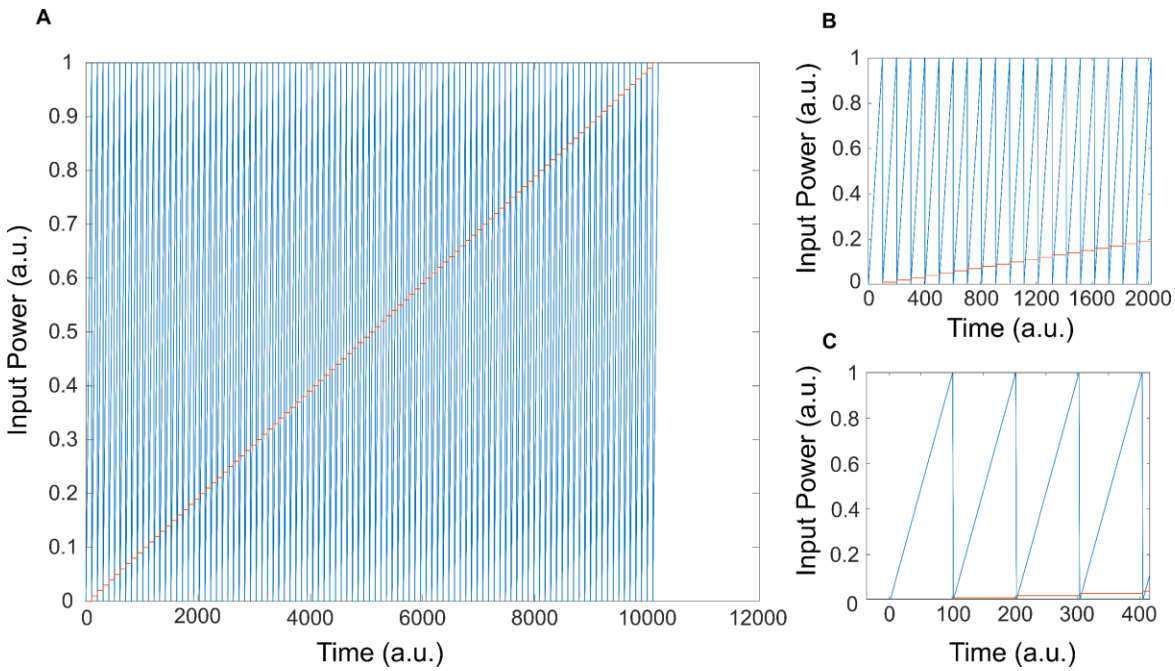

Fig. S4. Input power of control signals through the measurement. (**A**) Each control signal is assigned 101 power steps, control signal a (red line) moves one power step at every 101 time-steps while control signal b (blue line) will move one power steps at each time step. 10,201 addition events were measured through the experiment. (**B**, **C**) Zoomed-in view at selected time steps.

Fig. S5.

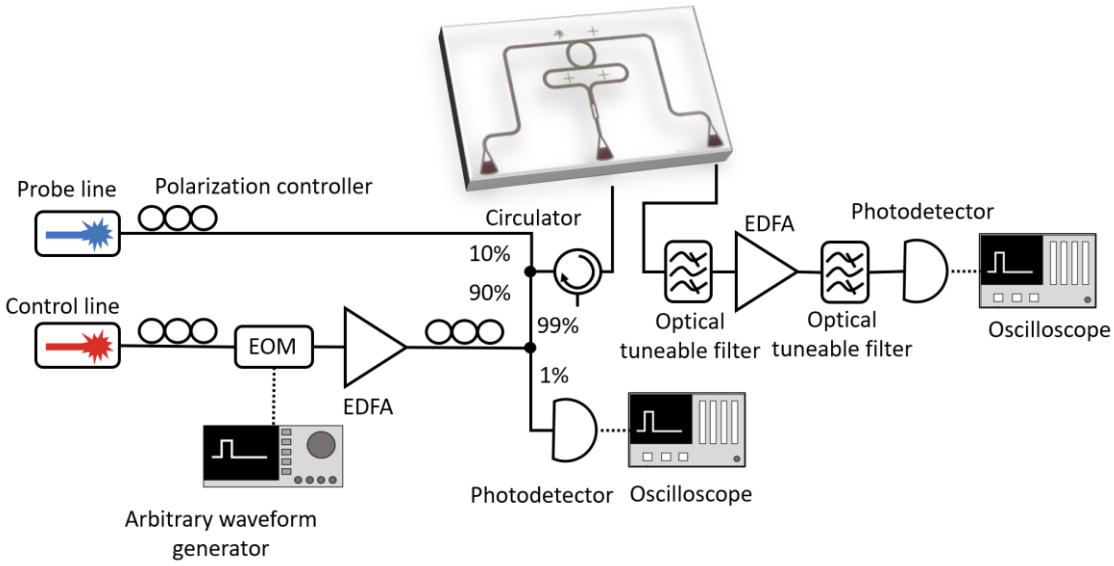

Fig. S5. Experiment set-up for time-scale response characterization.

Fig. S6.

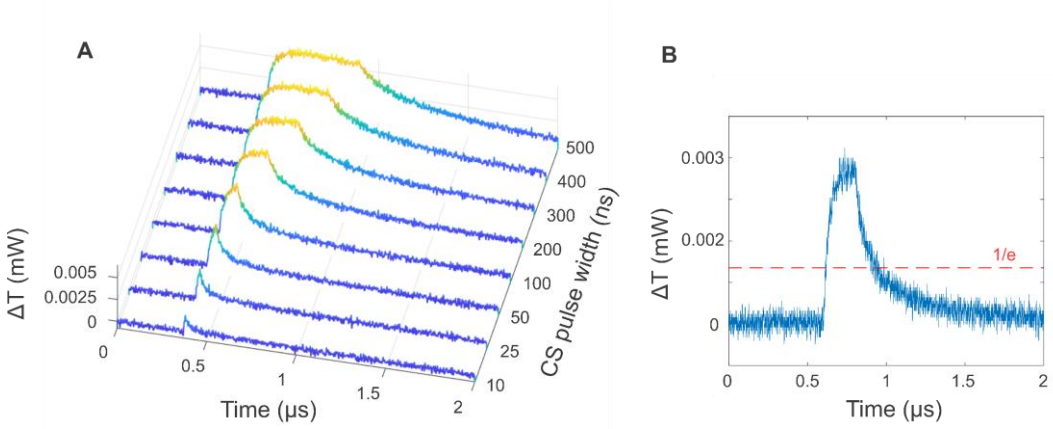

Fig. S6. **Square pulse response characterization.** (**A**) Transmission change at probe signal in response to input control signal with pulse width from 10 ns to 500 ns. (**B**) Leaky time constant τ (130 ns) is calculated as the time for output to decay to 1/e of its initial value when the input is removed. (Input CS pulse width: 200 ns)

Fig. S7.

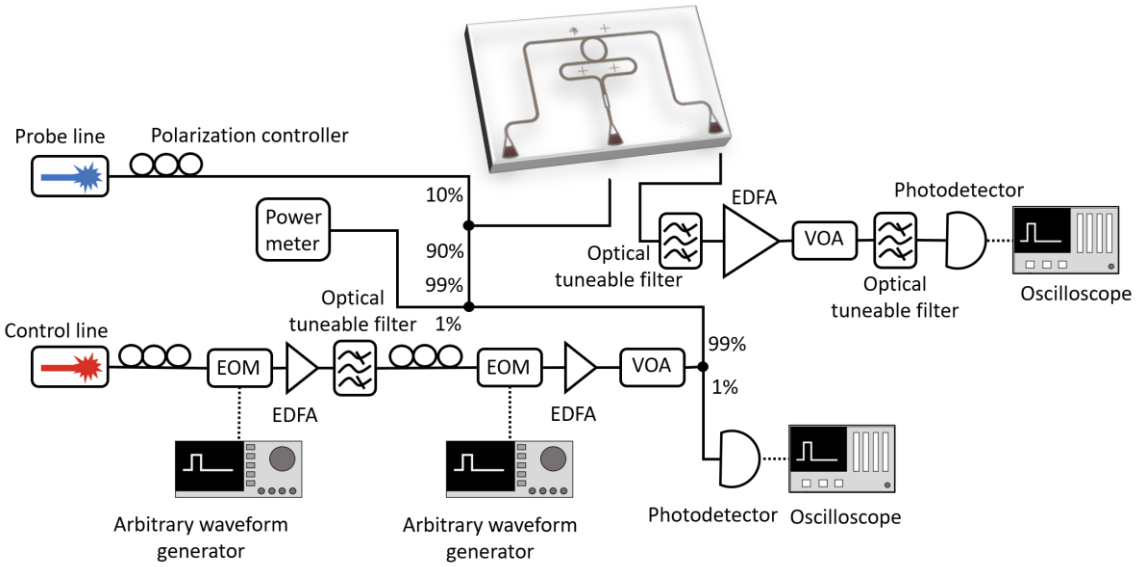

Fig. S7. Experiment set-up for integrating time-resolved signal.

Fig. S8.

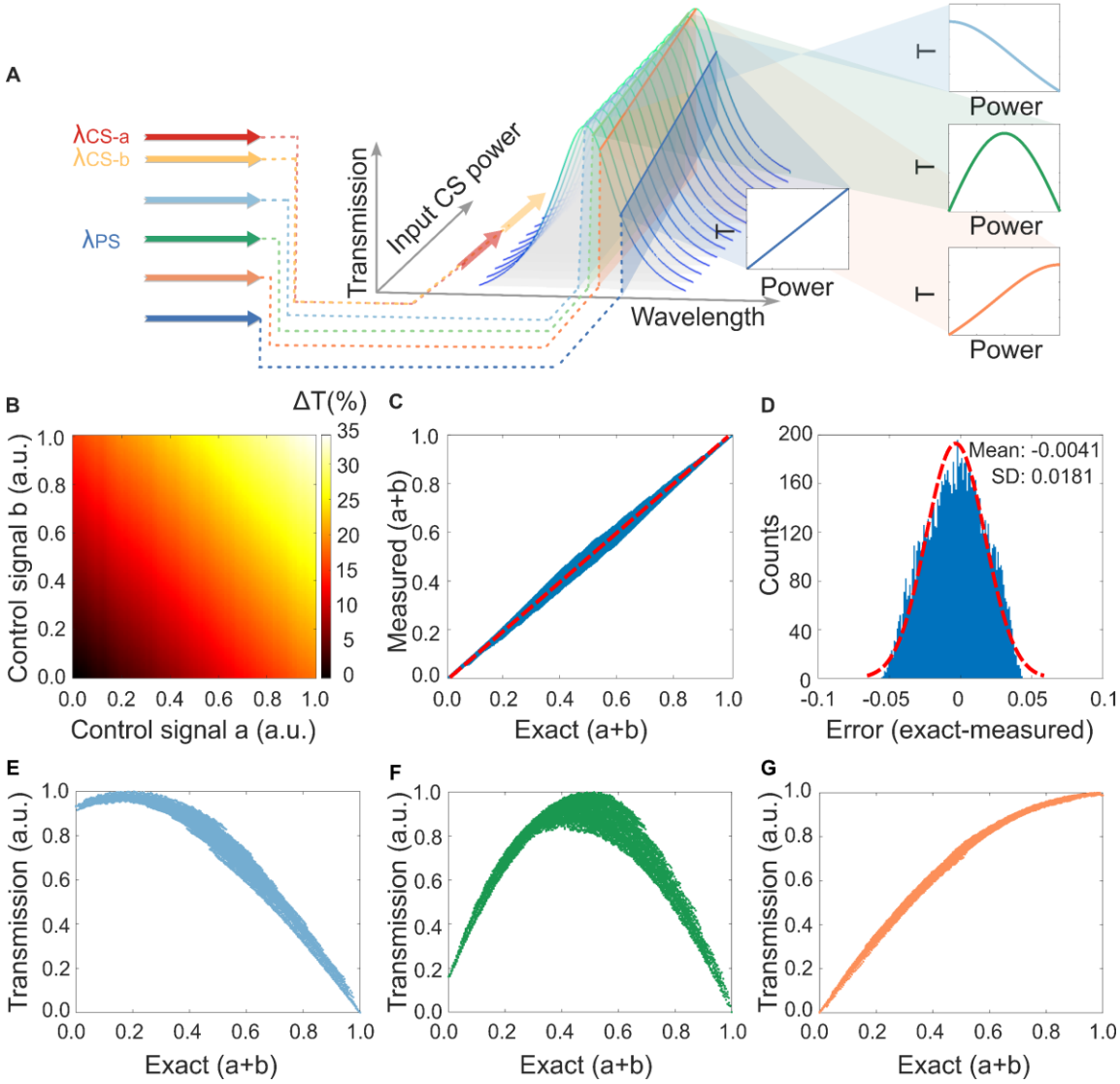

Fig. S8. **Across-wavelength accumulation with optically programmable transfer functions.** (**A)** Concept of the across-wavelength accumulation, where optical power of incoherent control signals is accumulated in heat, shifts the spectrum by thermo-optic effect, and encode onto the amplitude of a probe wavelength by selectively applying transfer function with exploring the spectrum shape of MRR. (**B**) Linear addition of signals carried by the intensity of two incoherent CS to the PS, and addition results are encoded within $\Delta T = (T - T_0)/ T_0$, which is the change in transmission of the level T with respect to the baseline T_0. (**C**) Measured addition results (calculated from normalized transmission variation in PS) compared with the expected condition. **D**) Error of the addition operation calculated from subtracting the measured addition results from the originally programmed addition results from 10210 addition events. **(E, F, G)** Non-linear functions applied on the across-wavelength summation results, obtained from different probe wavelengths in a single all-optical unit